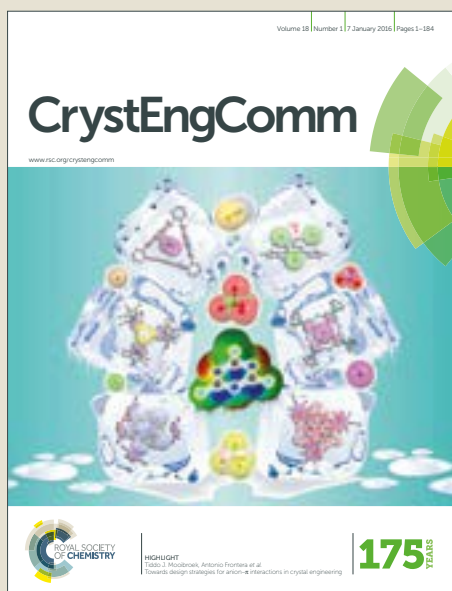


CrystEngComm

Accepted Manuscript



This article can be cited before page numbers have been issued, to do this please use: G. Ayoub, V. Strukil, L. Fábíán, C. Mottillo, H. Bao, Y. Murata, A. H. Moores, D. Margetic, M. Maksic and T. Friš, *CrystEngComm*, 2018, DOI: 10.1039/C8CE01727A.



This is an Accepted Manuscript, which has been through the Royal Society of Chemistry peer review process and has been accepted for publication.

Accepted Manuscripts are published online shortly after acceptance, before technical editing, formatting and proof reading. Using this free service, authors can make their results available to the community, in citable form, before we publish the edited article. We will replace this Accepted Manuscript with the edited and formatted Advance Article as soon as it is available.

You can find more information about Accepted Manuscripts in the [author guidelines](#).

Please note that technical editing may introduce minor changes to the text and/or graphics, which may alter content. The journal's standard [Terms & Conditions](#) and the ethical guidelines, outlined in our [author and reviewer resource centre](#), still apply. In no event shall the Royal Society of Chemistry be held responsible for any errors or omissions in this Accepted Manuscript or any consequences arising from the use of any information it contains.



Journal Name

COMMUNICATION

Mechanochemistry vs. solution growth: striking differences in bench stability of a cimetidine salt based on synthetic method

Received 00th January 20xx,
Accepted 00th January 20xx

DOI: 10.1039/x0xx00000x

www.rsc.org/

Ghada Ayoub,^a Vjekoslav Štrukil,^{b*} László Fábián,^c Cristina Mottillo,^a Huizhi Bao,^a Yasujiro Murata,^d Audrey Moores,^a Davor Margetić,^b Mirjana Eckert-Maksić^b and Tomislav Friščić^{a,b*}

Mechanochemically prepared solvated salt of the archetypal blockbuster drug cimetidine exhibits significantly different bench stability to analogous material made in solution. Samples obtained from solution are stable for weeks at room temperature and 45 °C, but mechanochemically made ones readily desolvate and convert to a new polymorph of non-solvated salt. While mechanochemistry is increasingly popular in synthesising drug solid forms, this work illustrates it can have a profound effect on material stability.

The discovery and preparation of new solid forms of active pharmaceutical ingredients (APIs)¹ is an important challenge of modern pharmaceutical materials science, with implications for improving physicochemical properties of drugs (*e.g.* solubility,² bioavailability,³ compressibility,⁴ dissolution rate,⁵ taste,⁶ colour⁷) and establishing new intellectual property.⁸

Mechanochemical⁹ techniques, *e.g.* liquid-assisted grinding (LAG) or polymer-assisted grinding (POLAG) have become of high interest in API solid form discovery and, since recently, API synthesis.^{10–13} This interest rests on short reaction times, and the ability to circumvent limitations of solubility, solvolysis or thermal degradation.^{14–17} Particularly notable is LAG, which uses a catalytic amount of a liquid to accelerate mechanochemical reactions and direct formation of polymorphs or stoichiometric variations of cocrystals or salts.^{1,18–23} While LAG reactions of molecular crystals are rapid, often enabling complete conversion in minutes,²⁴ they are also scalable to gram amounts in the laboratory.²⁵ In context of scale-up and manufacturing, twin screw extrusion now permits continuous mechanosynthesis of pharmaceutical cocrystals and organic molecules.²⁶ As mechanochemistry becomes increasingly significant in pharmaceutical materials science, most reports have focused on its efficiency in solid form

synthesis and discovery. In contrast, little or no attention has been paid to validating mechanochemical products, by identifying potential differences in their physicochemical properties compared to nominally identical materials obtained by solution techniques.

We now highlight the need for such critical validation of mechanochemically made materials by describing stark differences in bench stability of a mechanochemically prepared solvate of a salt of the API cimetidine²⁷ (**cim**) and fumaric acid (**H₂fum**) (Fig. 1a), compared to analogous material made from solution.

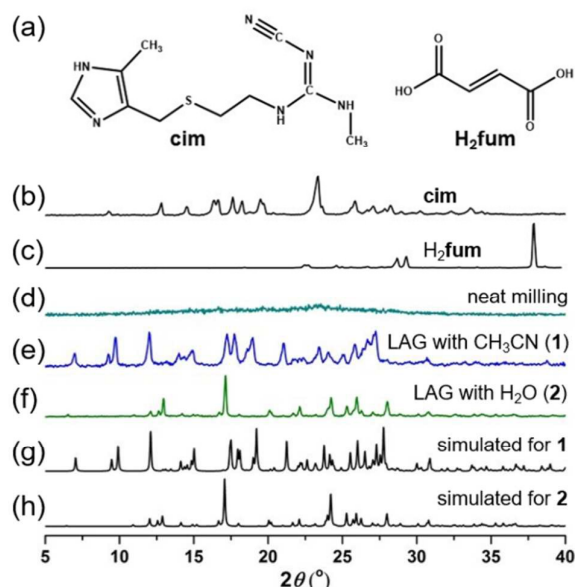


Figure 1. (a) Structures of **cim** and **H₂fum**. PXRD patterns for: (b) commercial **cim** and (c) **H₂fum**; (d) product of neat grinding of **cim** and **H₂fum**; (e) **1**, product of LAG with MeCN ($\eta=0.30$ $\mu\text{L}/\text{mg}$);²⁰ (f) **2**, product of LAG with water ($\eta=0.30$ $\mu\text{L}/\text{mg}$);²⁰ (g) simulated for crystal structure of **1** and (h) simulated for crystal structure of **2**.

Cimetidine (**cim**) is a well-known histamine H₂-receptor antagonist. Marketed as Tagamet, solid **cim** is of outstanding importance in pharmaceutical materials science as the first

^a Department of Chemistry, McGill University, Montreal, Quebec, Canada, H3A 0B8

^b Ruđer Bošković Institute, Bijenička cesta 54, Zagreb, Croatia, HR-10000.

^c School of Pharmacy, University of East Anglia, Norwich Research Park, Norwich, NR4 7TJ, United Kingdom

^d Institute for Chemical Research, Kyoto University, Uji, Kyoto 611-0011, Japan

*Corresponding authors: tomislav.friscic@mcgill.ca; vstrukil@irb.hr

Electronic Supplementary Information (ESI) available: Experimental procedures, TGA, FTIR-ATR, solid-state NMR, and SEM data. CCDC 1862747-1862749. See DOI: 10.1039/x0xx00000x

drug to reach \$1 billion in annual sales.^{27,28} It remains widely used in heartburn and peptic ulcer treatment, with recent work also indicating anti-cancer activity.²⁹ In contrast to its status as the pioneering beta-blocker and the archetype blockbuster drug, there have been no reports on crystal engineering of solid forms of **cim**, with existing structural studies dealing with polymorphs, the hydrochloride salt and metal complexes.³⁰

Neat milling of **cim** and H₂fum in a 1:1 stoichiometric ratio led to amorphization, as shown by a featureless powder X-ray diffraction (PXRD) pattern (Fig. 1). However, 20 minutes LAG with water or acetonitrile (MeCN) led to the disappearance of reactant X-ray reflections, and formation of new crystalline products. Using MeCN gave **1**, characterized by Bragg reflections distinct from those of any known forms of **cim** and H₂fum (Fig. 1).^{30,31} In contrast, the use of water gave a material (**2**) with a PXRD pattern different from that of **1** or any reported forms of **cim** and H₂fum (Fig. 1).

The crystal structure of **1** was determined by X-ray diffraction on crystals obtained by re-crystallisation of the mechanochemical product from MeCN (Fig. 2). Compound **1** is a solvated salt in which the asymmetric unit consists of singly protonated **cimH**⁺ cations, Hfum⁻ anions, as well as MeCN molecules disordered on a crystallographic inversion centre. Structural analysis and ¹H nuclear magnetic resonance (NMR) in DMSO-*d*₆ revealed that **1** contains **cim**, H₂fum and MeCN in a 1:1:0.5 respective ratio, consistent with the formula (**cimH**⁺)(Hfum⁻)·0.5MeCN. The structure is composed of cyclic hydrogen-bonded dimers of **cimH**⁺, held together by two N-H...N hydrogen bonds. The cationic dimers associate by N-H...O hydrogen bonds to chains of hydrogen-bonded Hfum⁻ anions that propagate along the crystallographic *b*-direction, forming a three-dimensional hydrogen-bonded structure. The ionic nature of **1** is confirmed by carbon-oxygen bond (C-O bond) lengths in Hfum⁻ anions. One of the carboxylate moieties on each anion exhibited very similar C-O bond distances 1.246(4) Å and 1.274(3) Å, consistent with a deprotonated carboxylate group, while the other exhibited one significantly shorter 1.212(4) Å and one longer 1.308(4) Å C-O bond, consistent with a neutral acid group. The acetonitrile molecule in the structure of **1** does not appear involved in any significant intermolecular interactions, except a potential C-H...N hydrogen bonding interaction (C...N separation 3.659(5) Å)³² between the nitrogen atom of the MeCN molecule and the methylene moiety in the 4-position of the imidazole ring of cimetidine (see ESI).

Attempts to obtain diffraction-quality crystals of **2** were unsuccessful, requiring structure characterisation from PXRD data (see ESI). Indexing of the PXRD pattern of **2**, after conversion to the conventional reduced cell, revealed a triclinic structure with *a*=7.8985 Å, *b*=8.3479 Å, *c*=14.2018 Å, α =87.575°, β =75.273°, γ =76.159° and volume of 879.2 Å³. Structure solution revealed **2** is a non-solvated salt of composition (**cimH**⁺)(Hfum⁻), with ionic nature of **1** and **2** confirmed by natural abundance ¹⁵N CP-MAS solid-state NMR spectra, which resembled those of **cim** hydrochloride, but were different from those of neutral **cim** (see ESI). The absence of solvent in **2** was also confirmed by thermogravimetric analysis (TGA, see ESI). Structure of **2** consists of layers in the crystallographic (001) plane, in which

cimH⁺ cations bridge parallel chains of hydrogen-bonded Hfum⁻ anions *via* N-H...O hydrogen bonds. The **cimH**⁺ cations in each layer form chains held by N-H...N hydrogen bonds, propagating in crystallographic [110]-direction (Figures 2c,d).

While samples of **1** prepared mechanochemically and from solution are nominally identical, they exhibit very different bench stability. Exposure of mechanochemically made **1** to 45°C over two days led to the disappearance of the prominent (1,0,-1) X-ray reflection at 2 θ =7.0° (Fig. 3). Identical behavior was observed regardless of the amount of acetonitrile used in LAG synthesis of **1**, as demonstrated by samples prepared at liquid-to-solid η ²⁰ ratios of 0.15, 0.30, 0.45 and 0.60 μ L/mg (see ESI).

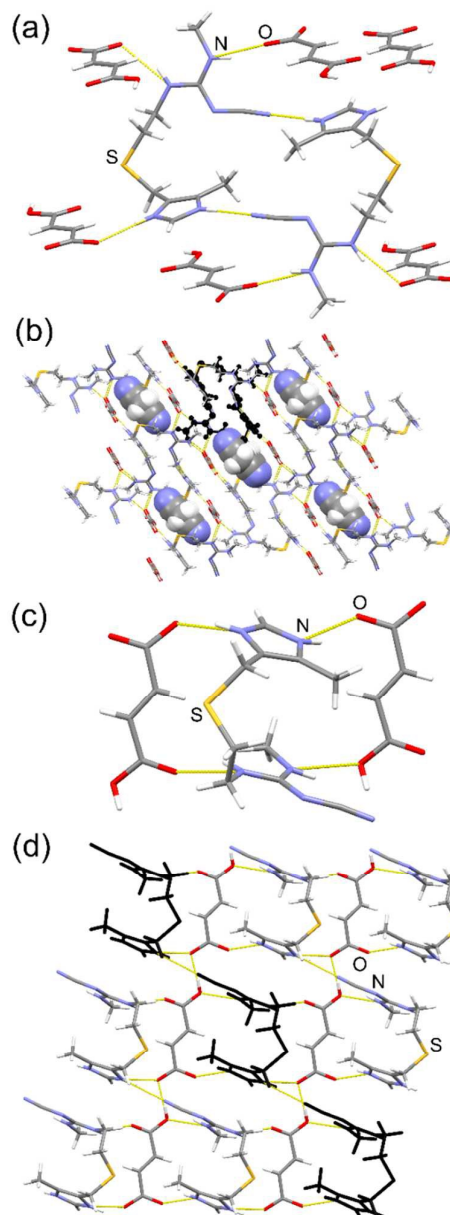


Figure 2. Crystal structures of **1** and **2**: (a) a single hydrogen-bonded dimer of **cimH**⁺ in **1**, associated to surrounding Hfum⁻ anions by N-H...O hydrogen bonds; (b) structure of **1** viewed along the crystallographic *b*-axis, with disordered acetonitrile guests shown in

a space-filling model, and one of the hydrogen-bonded cimH^+ dimers highlighted in black; (c) view of a single cimH^+ cation bridging neighboring Hfum^- anions via N-H...O bonds and (d) a single hydrogen-bonded layer in the structure of **2** viewed along the crystallographic c -axis, with a chain of hydrogen-bonded cimH^+ highlighted in black.

The remainder of the PXRD pattern changed less significantly, suggesting that the product (**1'**) is structurally similar to **1**. $^1\text{H-NMR}$ analysis of a solution of **1'** in $\text{DMSO-}d_6$ revealed the absence of MeCN and composition $(\text{cimH}^+)(\text{Hfum}^-)$, identical to **2**. Scanning electron microscopy (SEM) showed that mechanochemically made **1** consisted of elongated cuboid particles with a length of 228 ± 85 nm (Fig. 3g). After thermal desolvation, little change in particle size or morphology was observed, consistent with retention of crystallinity (Figure 3g,h).

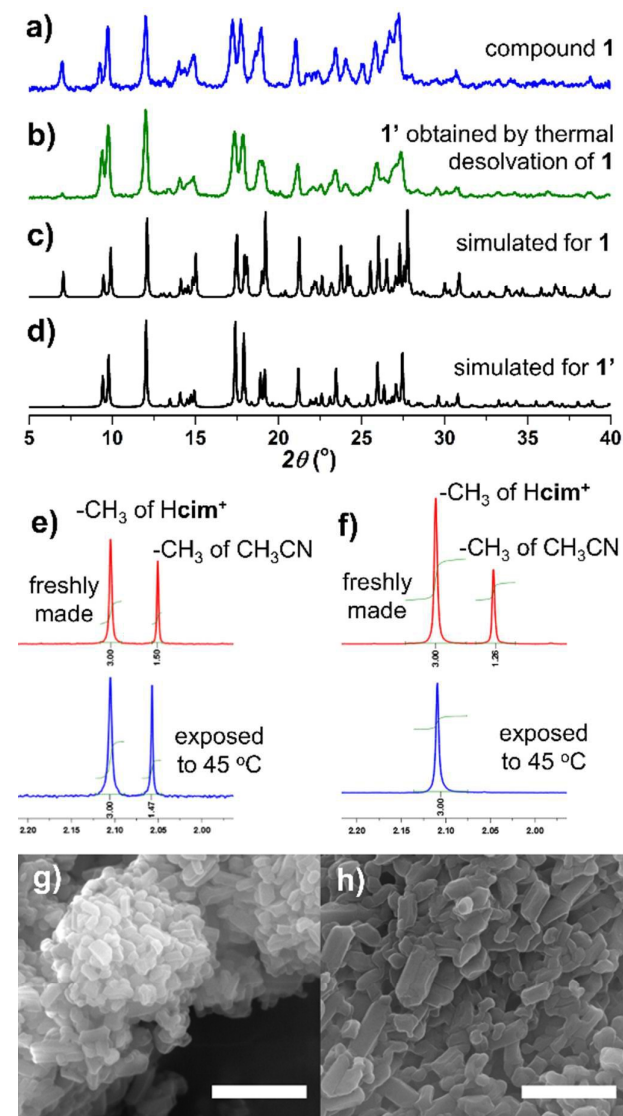


Figure 3. Analysis of **1** before and after two days at 45°C in air. PXRD patterns for: (a) mechanochemically made sample; (b) mechanochemically made sample after exposure to 45°C ; (c) simulated for **1** and (d) for **1'**. Section of $^1\text{H-NMR}$ spectrum recorded in $\text{DMSO-}d_6$ for (e) solution-made **1** before (top) and after thermal treatment (bottom) and (f) mechanochemically made **1** before (top) and after exposure to 45°C (bottom).

SEM images for mechanochemically made **1** (g) before and (h) after exposure to 45°C . Scale bar corresponds to $1\ \mu\text{m}$.

Indexing of PXRD data for **1'** revealed a monoclinic unit cell strongly resembling that of **1**, with $a=13.770(1)\ \text{\AA}$, $b=8.0432(5)\ \text{\AA}$, $c=18.949(1)\ \text{\AA}$, $\beta=107.419(4)^\circ$ and $V=2002.48(21)\ \text{\AA}^3$. Simulated annealing structure solution and Rietveld refinement in space group $P2_1/n$ confirmed that **1'** is indeed a polymorph of the non-solvated salt **2**, isostructural to **1** (Figure 4a, also see ESI). The absence of solvent in **1'** was also verified by TGA (see ESI). Crystal structure analysis readily explains the significant reduction in intensity of the (1,0,-1)-reflection upon desolvation of **1** into **1'**: the (1,0,-1)-planes of **1** are populated with guest MeCN molecules, and their removal leads to formation of voids illustrated in Figure 4b, and a reduction in electron density contributing to X-ray scattering from those crystal planes.

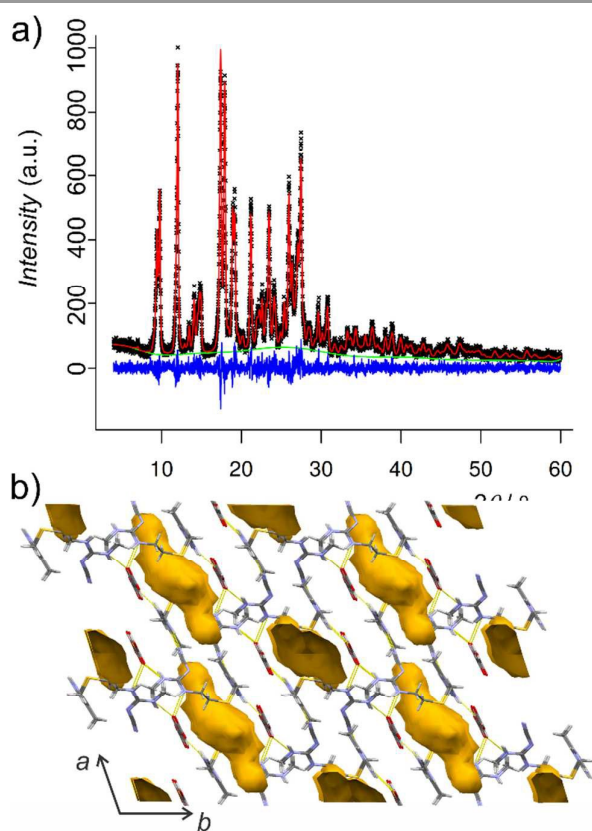


Figure 4. a) Final Rietveld fit for the structure of **1'** determined from PXRD data and b) crystal structure of **1'** viewed parallel to the crystallographic b -axis and displaying the voids (yellow, detected by a spherical probe of $1.2\ \text{\AA}$ radius) previously occupied by MeCN guests.

In contrast, solution-made **1** was significantly more resistant to thermal treatment. Crystal structure analysis of a single crystal of **1**, after being kept at 45°C for two days revealed no evidence of acetonitrile loss. This was corroborated by solution $^1\text{H-NMR}$ analysis of thermally treated crystals, which revealed the loss of less than 10% of the initial amount of MeCN. Similarly, no significant difference was observed in

crystallographic unit cell parameters or overall appearance of X-ray diffraction spots of **1** upon exposure to 45 °C over a period of 5 and 10 days (see ESI).

Table 1. Crystallographic parameters for a single crystal of **1** after exposure to 45 °C for 0, 5 and 10 days.

<i>t</i> / days	<i>a</i> / Å	<i>b</i> / Å	<i>c</i> / Å	β / °
0	13.804(1)	8.0191(7)	18.715(2)	107.580(3)
5	13.799(1)	8.0172(7)	18.723(2)	107.657(3)
10	13.792(1)	8.0148(7)	18.726(2)	107.555(3)

The striking difference in stability of mechanochemically- and solution-made **1** is even more evident from ¹H-NMR monitoring of MeCN content in samples exposed to air at room temperature (Figures 5a,b). Mechanochemically made **1** lost almost all MeCN within 40 h, while solution-grown crystals remained solvated even after 15 days. Indeed, complete removal of MeCN from solution-grown **1** was difficult even upon harsher treatment: after exposure to 80 °C and reduced pressure of 0.2 bar for 10 days, ¹H-NMR analysis still revealed the presence of 0.15 molecules of MeCN per each (cimH⁺)(Hfum⁻) unit. The most likely explanation for the observed stability differences is particle size. As revealed by SEM, solution-growth crystals of **1** are much larger than mechanochemical ones, appearing as needles with a length on the order of 1 mm (Fig. 5). To qualitatively evaluate the effect of crystal size, we studied the effect of mechanical treatment on solution-grown **1**, by either gentle or vigorous grinding using a mortar and pestle.

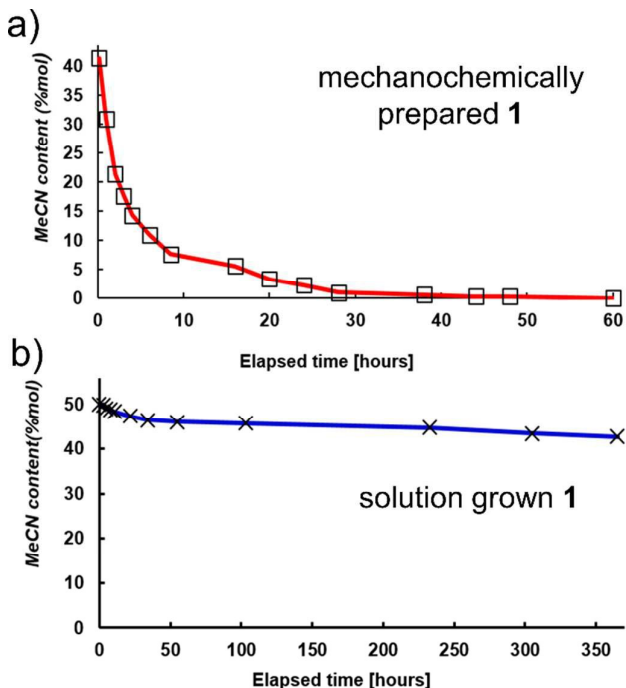


Figure 5. Difference in rates of acetonitrile (MeCN) loss in open air, at room temperature, for samples of **1** that were: a) mechanochemically prepared and b) solution grown.

SEM analysis revealed that gentle grinding fragmented the crystals into smaller particles of average size around 230 μm in length, while harsher grinding led to average size of ca. 19 μm (see ESI). After 2 days at 45 °C in open air, the gently ground sample underwent more significant MeCN loss (50% of original content) compared to unperturbed crystals (2%). Sample produced by harsher grinding lost ca. 78% of original MeCN content, resulting in a material of composition (cimH⁺)(Hfum⁻)·0.11 MeCN. These results, summarized in the Table S1 in the ESI, support the view that stability differences between mechanochemically and solution-grown **1** are likely due to different particle size and defects.^{33,34}

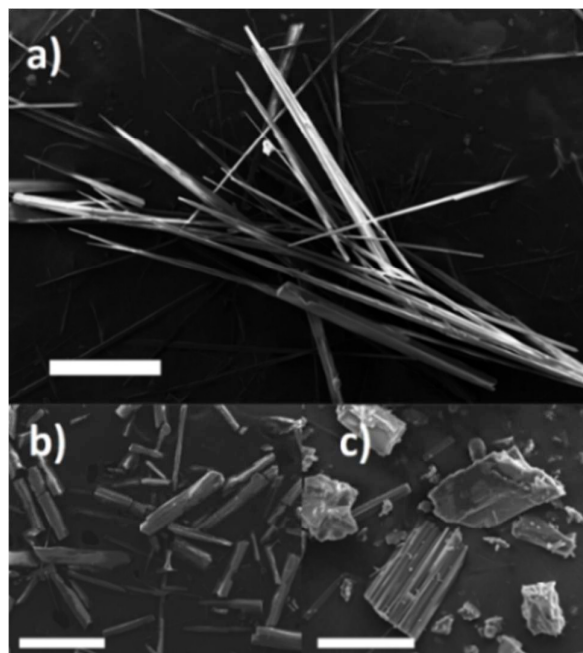


Figure 6. SEM images for: (a) solution grown crystals of **1** (scalebar = 400 μm); (b) solution grown crystals of **1** after gentle grinding (scalebar = 400 μm) and (c) harsher grinding using a mortar and pestle (scalebar = 40 μm).

In summary, we described a significant difference in stability between nominally identical solid forms of cimetidine, prepared by mechanochemistry or solution growth. So far, studies of mechanochemical synthesis of API solid forms have focused on screening and quantitative synthesis. However, this work highlights a not yet explored effect^{33,34} of mechanochemistry on solid-state properties of solid API forms. While this effect herein led to the discovery of a new polymorph of a previously not described salt solid form of cimetidine, in a wider context it can be regarded as a potential problem when mechanochemical techniques are employed. Consequently, this work highlights a growing need to investigate and validate properties of mechanochemically made materials with respect to analogous ones made by different methods.

Acknowledgments

We thank the Unity Through Knowledge fund (project no. 63/10), NSERC Discovery Grant (RGPIN-2017-06467), E. W. R.

Steacie Memorial Fellowship (SMFSU 507347-17). GA acknowledges the Ludo Frevel Crystallography Scholarship and McGill University Departmental Fellowship. We thank Prof. J. Bernstein for advice and critical reading of the manuscript, and Drs. Fred Morin and Robin S. Stein for acquiring solid-state NMR data.

Notes and references

- a) N. K. Duggirala, M. L. Perry, Ö. Almarsson and M. J. Zaworotko *Chem. Commun.* 2016, **52**, 640; b) D. J. Berry and J. W. Steed *Chem. Commun.* 2017, **117**, 3; c) P. C. Vioglio, M. R. Chierotti and R. Gobetto *Adv. Drug. Rev.* 2017, **117**, 86; d) J. F. Willart, V. Caron, R. Lefort, F. Danède, D. Prévost, M. Descamps, *Solid State Commun.* 2004, **132**, 693; e) S. Domingos, V. André, S. Quaresma, I. C. B. Martins, M. F. Minas de Piedade and M. T. Duarte *J. Pharm. Pharmacol.* 2015, **67**, 830; f) G. Ramon, K. Davies, L. R. Nassimbeni, *CrystEngComm*, 2014, **16**, 5802; g) T. Friščić, W. Jones, *J. Pharm. Pharmacol.*, 2010, **62**, 1547; h) D. A. Hirsh, A. J. Rossini, L. Emsley and R. W. Schurko *Phys. Chem. Chem. Phys.* 2016, **18**, 25893.
- a) D. P. Elder, R. Holm, H. Lopez de Diego, *Int. J. Pharm.*, 2013, **453**, 88; b) D. J. Good and N. Rodríguez-Hornedo *Cryst. Growth Des.* 2009, **9**, 2252.
- D. P. McNamara, S. L. Childs, J. Giordano, A. Iarriccio, J. Cassidy, M. S. Shet, R. Mannion, E. O'Donnell, A. Park, *Pharm. Res.*, 2006, **23**, 1888.
- a) D.-K. Bučar, J. A. Elliott, M. D. Eddleston, J. K. Cockcroft and W. Jones *Angew. Chem. Int. Ed.* 2015, **54**, 249; b) S. Karki, T. Friščić, L. Fábrián, P. R. Laity, G. M. Day, W. Jones, *Adv. Mater.*, 2009, **21**, 3905.
- M. Žegarac, E. Lekšić, P. Šket, J. Plavec, M. D. Bogdanović, D.-K. Bučar, M. Dumić, E. Meštović, *CrystEngComm*, 2014, **16**, 32.
- A. R. Patel, P. R. Vavia, *AAPS PharmSciTech.*, 2008, **9**, 544.
- D.-K. Bučar, S. Filip, M. Arhangelskis, G. O. Lloyd, W. Jones, *CrystEngComm*, 2013, **15**, 6289.
- A. V. Trask, *Mol. Pharm.*, 2007, **4**, 301.
- S. L. James, C. J. Adams, C. Bolm, D. Braga, P. Collier, T. Friščić, F. Grepioni, K. D. M. Harris, G. Hyett, W. Jones, A. Krebs, J. Mack, L. Maini, A. G. Orpen, I. P. Parkin, W. C. Shearouse, J. W. Steed, D. C. Waddell, *Chem. Soc. Rev.* 2012, **41**, 413.
- S. L. Childs, N. Rodríguez-Hornedo, L. S. Reddy, A. Jayasankar, C. Maheshwari, L. McCausland, R. Shipplett, B. C. Stahly, *CrystEngComm*, 2008, **10**, 856.
- D. Braga, L. Maini, F. Grepioni *Chem. Soc. Rev.* 2013, **42**, 7638.
- a) D. Tan, L. Loots, T. Friščić *Chem. Commun.* 2016, **52**, 7760; b) L. Konnert, F. Lamaty, J. Martinez and E. Colacino *Chem. Rev.* 2017, **117**, 13757.
- Y. Zhou, F. Guo, C. E. Hughes, D. L. Browne, T. R. Peskett, K. D. M. Harris, *Cryst. Growth Des.* 2015, **15**, 2901.
- D. Hasa, G. Schneider Rauber, D. Voinovich, W. Jones, *Angew. Chem. Int. Ed.* 2015, **54**, 7371.
- D.-K. Bučar, J. A. Elliott, M. D. Eddleston, J. K. Cockcroft, W. Jones, *Angew. Chem. Int. Ed.* 2015, **54**, 249.
- E. Lu, N. Rodríguez-Hornedo, R. Suryanarayanan, *CrystEngComm*, 2008, **10**, 665.
- D. J. Berry, C. C. Seaton, W. Clegg, R. W. Harrington, S. J. Coles, P. N. Horton, M. B. Hursthouse, R. Storey, W. Jones, T. Friščić, N. Blagden, *Cryst. Growth Des.*, 2008, **8**, 1697.
- T. Friščić, *J. Mater. Chem.* 2010, **20**, 7599.
- W. Jones, M. D. Eddleston, *Faraday Discuss.*, 2014, **170**, 9.
- T. Friščić, S. L. Childs, S. A. A. Rizvi, W. Jones, *CrystEngComm*, 2009, **11**, 418.
- A. V. Trask, W. D. S. Motherwell, W. Jones, *Chem Commun.* 2004, 890.
- T. Friščić, A. V. Trask, W. Jones, W. D. S. Motherwell, *Angew. Chem. Int. Ed.* 2006, **45**, 7546.
- R. Banerjee, P. M. Bhatt, N. V. Ravindra, G. R. Desiraju, *Cryst. Growth Des.*, 2005, **5**, 2299.
- K. L. Nguyen, T. Friščić, G. M. Day, L. F. Gladden, W. Jones, *Nat. Mater.*, 2007, **6**, 206.
- X. Ma, G. K. Lim, K. D. M. Harris, D. C. Apperley, P. N. Horton, M. B. Hursthouse, S. L. James, *Cryst. Growth Des.*, 2012, **12**, 5869.
- D. Daurio, C. Medina, R. Saw, K. Nagapudi, F. Alvarez-Núñez, *Pharmaceutics*, 2011, **3**, 582.
- R. W. Brimblecombe, W. A. M. Duncan, G. J. Durant, J. C. Emmett, C. R. Ganellin, G. B. Leslie, M. E. Parsons, *Gastroenterology*, 1978, **74**, 339.
- M. Freemantle, *Chem. Eng. News.* 2005, **83**, 118.
- a) Y. Zheng, M. Xu, X. Li, J. Jia, K. Fan and G. Lai *Mol. Immun.* 2013, **54**, 74; b) P. Pantziarka, G. Bouche, L. Meheus, V. Sukhatme, V. P. Sukhatme, *ecancer* 2014, **8**:485.
- a) D. A. Middleton, C. S. Le Duff, X. Peng, D. G. Reid, D. Saunders, *J. Am. Chem. Soc.*, 2000, **122**, 1161; b) A. S. Tatton, T. N. Pham, F. G. Vogt, D. Iuga, A. J. Edwards, S. P. Brown, *CrystEngComm*, 2012, **14**, 2654; c) A. E. Watts, K. Maruyoshi, C. E. Hughes, S. P. Brown, K. D. M. Harris, *Cryst. Growth Des.*, 2016, **16**, 1798; d) F. T. Greenaway, L. M. Brown, J. C. Dabrowiak, M. R. Thompson, V. M. Day, *J. Am. Chem. Soc.*, 1980, **102**, 7782.
- The Cambridge Structural Database (CSD) contains 17 entries involving the cimetidine backbone, including cimetidinium hydrochloride (EHIWEZ), cimetidinium hydrochloride monohydrate (CADVIM), cimetidine monohydrate (CIMGUA), three polymorphs (CIMETD, CIMETD01, CIMETD02, CIMETD03, CIMETD04), five Cu²⁺ (CMTCUA, CONYUZ, CONYUZ01, DEFWEQ, GEWYUC), two Ni²⁺ (DOKGEP, GAXVUW), Pt²⁺ (INOPEG) and Co²⁺ (DOKGAL) complexes.
- Evaluated using PLATON: A. L. Spek, *Acta Cryst.* 2009, **D65**, 148.
- For a study how particle size can affect relative stabilities of polymorphs formed by mechanochemistry, see: A. M. Belenguer, G. I. Lampronti, A. J. Cruz-Cabeza, C. A. Hunter, J. K. M. Sanders *Chem. Sci.* 2016, **7**, 6617.
- For a comparison of thermodynamic stability of a material prepared mechanochemically, through accelerated aging and solution techniques, see: Z. Akimbekov, A. D. Katsenis, G. P. Nagabushana, G. Ayoub, M. Arhangelskis, A. J. Morris, T. Friščić and A. Navrotsky, *J. Am. Chem. Soc.* 2017, **139**, 7952.

Electronic Supplementary Information

Mechanochemistry vs. solution growth: striking differences in bench stability of a cimetidine salt based on synthetic method

Ghada Ayoub, Vjekoslav Štrukil,* László Fábián, Cristina Mottillo, Huizhi Bao, Yasujiro Murata, Audrey Moores, Davor Margetić, Mirjana Eckert-Maksić, and Tomislav Friščić*

Experimental details

General details

Reagents cimetidine (**cim**), cimetidine hydrochloride salt (**cim**·HCl), and fumaric acid (**H₂fum**) were purchased from Sigma Aldrich (St. Louis, MO, USA) and used without modification. Acetonitrile (ACS certified) was purchased from Fisher Scientific (Waltham, MA USA).

Instrumentation

Single crystal X-ray diffraction

The crystal structure of (**cim**H⁺)(**Hfum**⁻)·0.50 MeCN (**1**) was collected on a Bruker D8 Advance diffractometer (Bruker-AXS, Madison, WI, USA) with a Photon 100 CMOS area detector and an I μ S microfocus X-ray source (Bruker AXS) using Cu-K α ($\lambda=1.54060$ Å) radiation. Crystals were coated with Paratone oil (Hampton Research, Aliso Viejo, CA, USA) and cooled to 100 K under a cold stream of nitrogen using an Oxford cryostat (Oxford Cryosystems, Oxford, UK). The structures were determined by least squares refinement against F^2 using SHELX-2014¹ software running under the WinGX user interface. Non-hydrogen atoms were located from the difference map and refined anisotropically. All hydrogen atom coordinates and thermal parameters were constrained to ride on the carrier atoms. The acetonitrile was located on centre of inversion and it was successfully modeled with partial occupancy.

Powder X-ray diffraction (PXRD)

Powder X-ray diffraction patterns were collected using a Bruker D2 powder diffractometer equipped with a CuK α ($\lambda=1.54060$ Å) source and Lynxeye detector (Bruker AXS, Madison, WI) with a lower and upper discriminant of 0.110 V and 0.250 V respectively. The patterns were collected in the range of 5° to 40°. Analysis of PXRD patterns was conducted using Panalytical X'Pert Highscore Plus software. Experimental patterns were compared to simulated patterns calculated from single crystal structures using Mercury software package.

Fourier-transform infrared attenuated total reflection (FTIR-ATR)

All FTIR-ATR spectra were collected in the solid state using a Bruker Vertex 70 FTIR-ATR spectrometer (Milton, ON, CA) in the range of 4000 cm⁻¹ to 400 cm⁻¹. FTIR spectra were analysed using Bruker OPUS software.

Thermogravimetric analysis (TGA)

Thermograms were collected using a TA Instruments TGA Q500 thermogravimetric analyser at a heating rate of 10°C/min from 25°C to 700°C under dynamic atmosphere of nitrogen and air. The flow rates of the

purge gas and sample gas were set at 50 mL/min and 50 mL/min respectively. TGA curves were analyzed with TA Universal Analysis software.

Solid-state ^{15}N CP-MAS NMR (ssNMR)

Natural abundance ^{15}N ssNMR spectra were collected on a Varian VNMRS NMR spectrometer (Palo Alto, CA, USA) operating at a ^1H frequency of 399.77 MHz and an ^{15}N frequency of 40.53 MHz using a 7.5 mm double-resonance Varian T3 probe. All spectra were collected at a spin rate of 5 kHz using cross-polarization with a contact time of 1.5 ms and a recycle delay ranging between 2 s and 20 s. Spectra were referenced using glycine at -347.1 ppm with respect to CH_3NO_2 . NMR spectra were analysed using MestreNova software.

Solution NMR Spectroscopy

All ^1H NMR solution spectra (Bruker Optics Ltd, Milton, ON, Canada) were collected using $\text{DMSO-}d_6$ as the solvent, on a Bruker 400 MHz spectrometer and interpreted using MestreNova software. The samples were dissolved in one ampule of $\text{DMSO-}d_6$.

Synthesis of the salts

$(\text{Hcim}^+)(\text{Hfum}^-) \cdot 0.50 \text{ MeCN}$ (compound 1)

Cimetidine (0.54 mmol, 137 mg) and fumaric acid (0.54 mmol, 63 mg) were milled in a stainless-steel jar in the presence of acetonitrile (60 μL) on a Retsch MM400 shaker mill for 30 minutes. The salt solvate was characterized by PXRD, TGA, and FTIR-ATR.

Single crystals suitable for single crystal X-ray diffraction were obtained by slow evaporation of a solution in MeCN.

$(\text{Hcim}^+)(\text{Hfum}^-)$ made by milling (compound 2)

Cimetidine (0.54 mmol, 137 mg) and fumaric acid (0.54 mmol, 63 mg) were milled in a stainless-steel jar in the presence of water (60 μL) as a liquid additive on a Retsch MM400 mill for 30 minutes. The product was characterized by PXRD, TGA, and FTIR-ATR. The crystal structure of the salt was solved and refined from PXRD using Rietveld refinement technique.

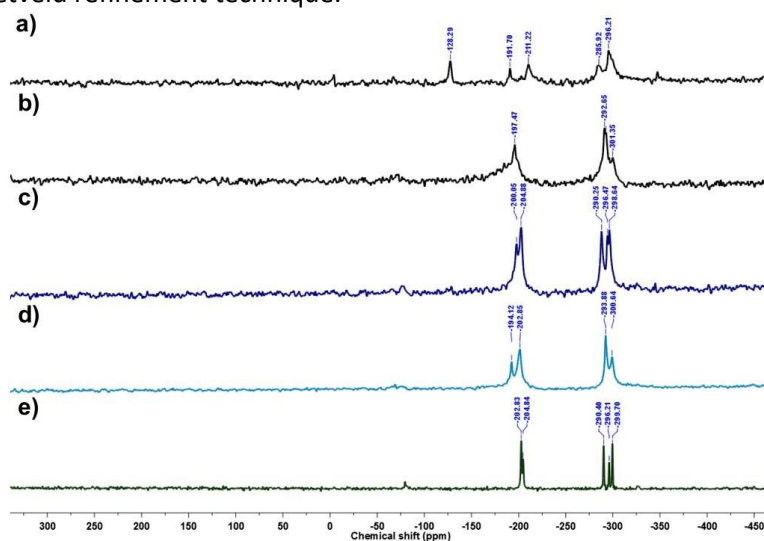


Figure S1. Solid-state ^{15}N CP-MAS NMR spectra of commercially available (a) **cim**, (b) **cimH⁺Cl⁻** salt, (c) **(cimH⁺)(Hfum⁻) · 0.50 MeCN** (compound 1), (d) **(cimH⁺)(Hfum⁻)** made mechanochemically (compound 2) and (e) **(cimH⁺)(Hfum⁻)** made by desolvation of 1 (compound 1'). The similarity in the spectra between (b), (c), (d) and (e) confirms that compounds 1, 2 and 1' are salts.

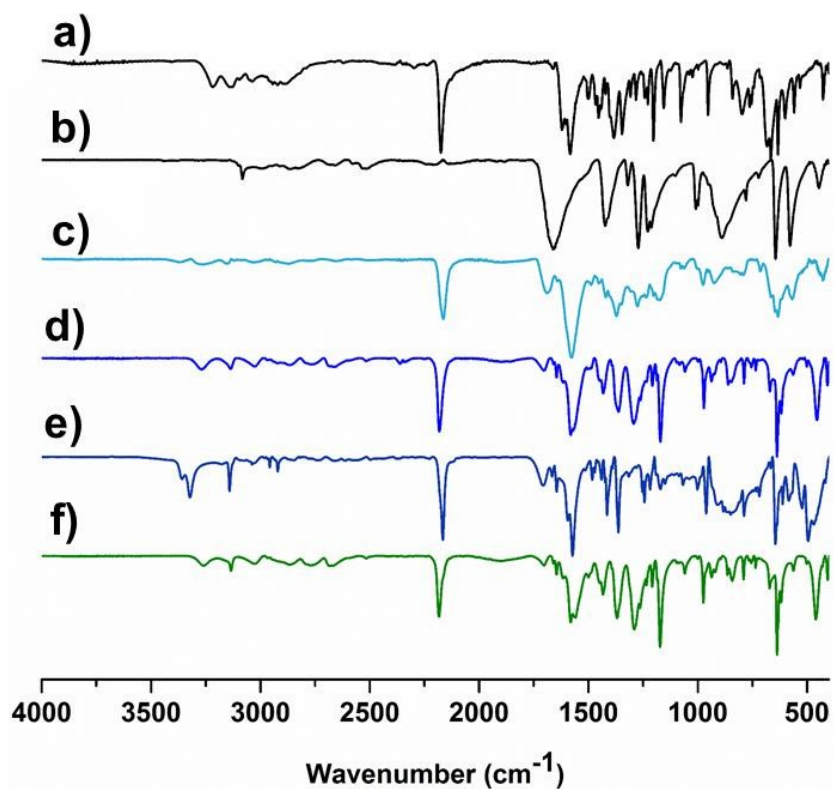


Figure S2. FTIR-ATR spectra for: (a) **cim**, (b) **H₂fum**, (c) neat milling of **cim** and **H₂fum**, (d) compound **1** formed by milling **cim** and **H₂fum** in the presence of MeCN as a liquid additive, (e) compound **2** formed by milling **cim** and **H₂fum** in the presence of water as a liquid additive, (f) compound **1'** obtained by desolvation of mechanochemically prepared compound **1**.

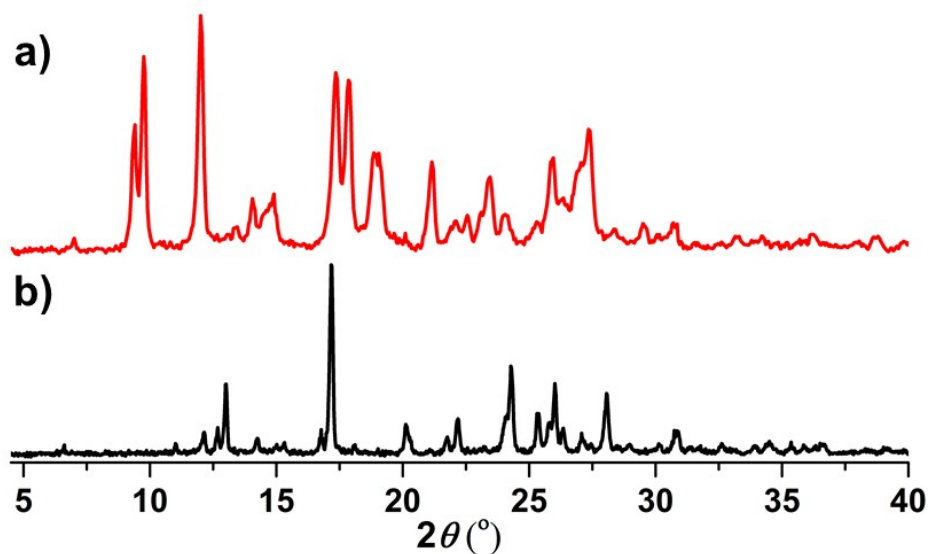


Figure S3. Polymorphs of (**Hcim**⁺)(**Hfum**⁻) salt generated by: (a) heating form **1** for two days at 45 °C to yield **1'** and (b) milling **cim** and **H₂fum** in the presence of water as a LAG to yield **2**.

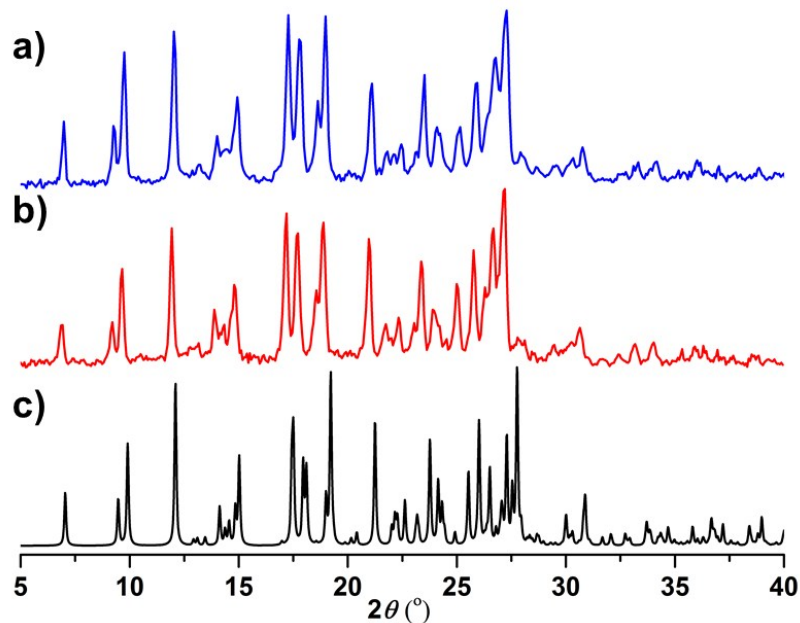


Figure S4. Comparison of PXRD patterns of **1** prepared by: (a) solution synthesis, (b) mechano-synthesis, c) simulated for the crystal structure of **1**.

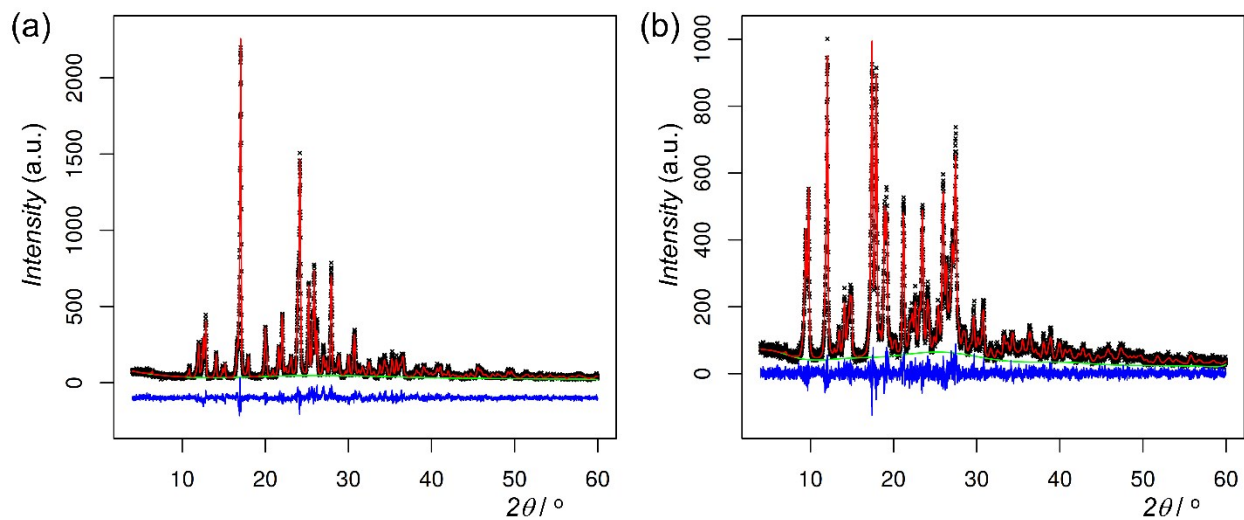


Figure S5. Final Rietveld fit for the structures of (a) compound **2** and (b) compound **1'**, determined from PXRD data.

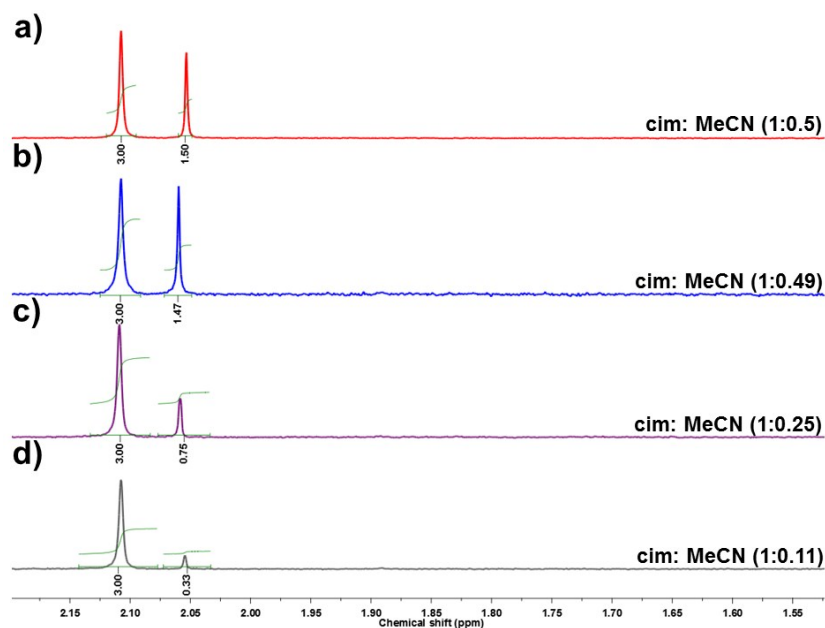


Figure S6. High field portion of ^1H -NMR spectra of single crystals of **1**: a) freshly prepared from MeCN solution, b) kept at 45°C for two days, c) gently ground and kept for 2 days at 45°C for two days and d) harshly ground and kept for 2 days at 45°C .

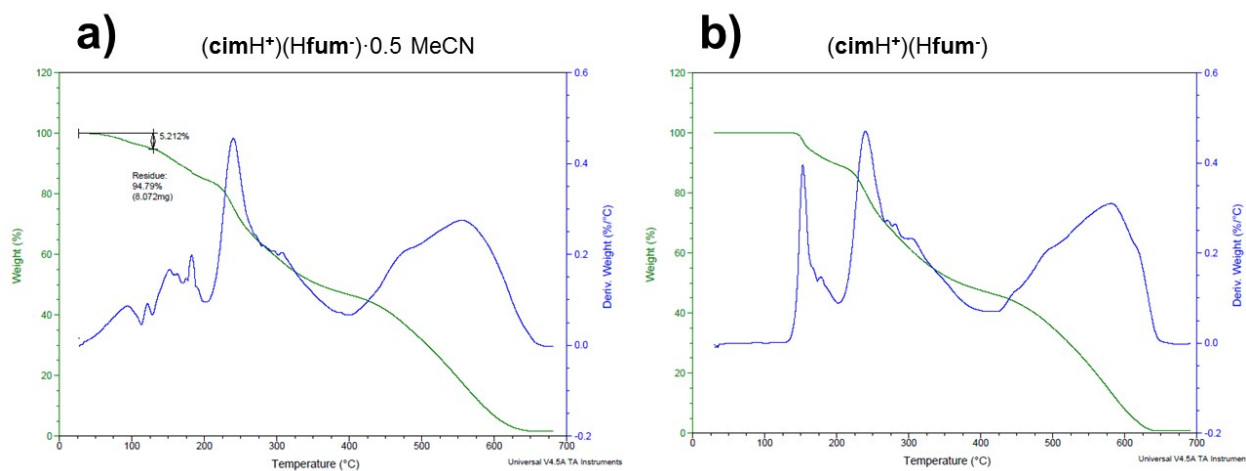


Figure S7. TGA thermograms of: a) compound **1** and b) compound **2**. The first step in a) corresponds to the weight loss of ca 5 wt%, which matches the theoretically calculated weight content of MeCN in the solvated salt **1** (5.2%). Notably, the step does not appear in the TGA thermogram of the nonsolvated compound **2** shown in b).

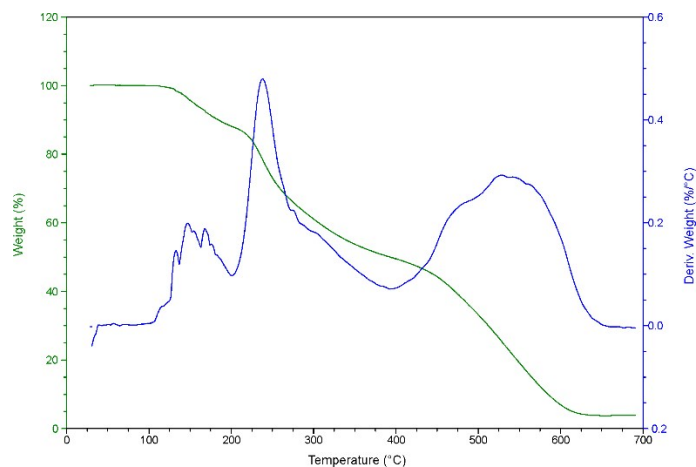


Figure S8. TGA thermogram of compound **1'**. In contrast to compound **1**, no weight loss is observed below 100 °C, and the thermogram is similar to that of the non-solvated salt **2**.

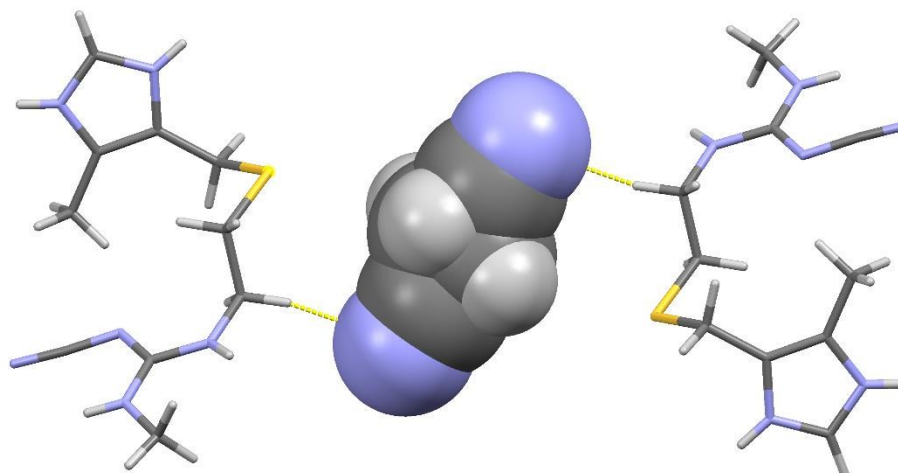


Figure S9. View of the disordered guest molecule of acetonitrile (shown in space-filling) in the crystal structure of **1**, illustrating C-H...N interactions (C...N separation 3.66 Å, C-H...N angle 165°) to neighboring **cimH⁺**.

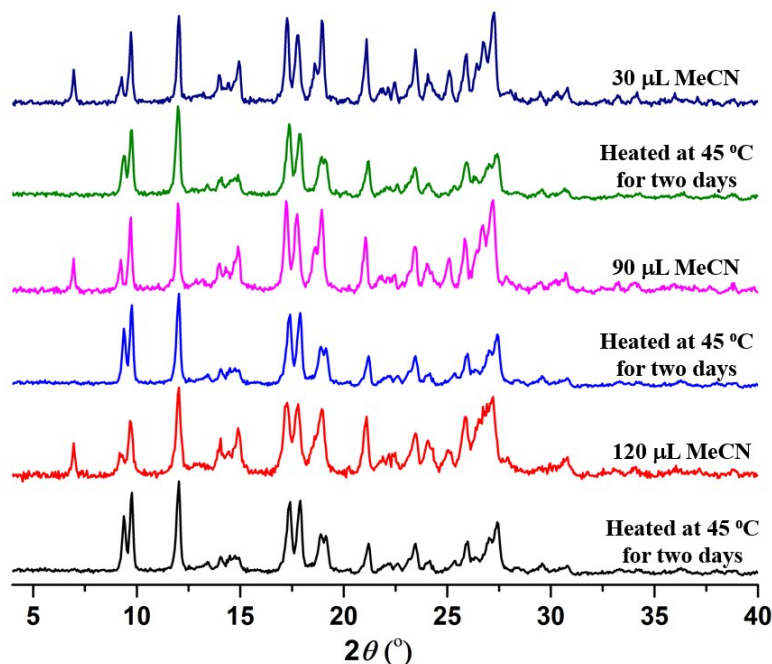


Figure S10. Comparison of PXRD patterns for samples of **1** mechanochemically prepared using different amounts of MeCN as the LAG additive, fresh and after exposure to 45 $^{\circ}\text{C}$ over 2 days.

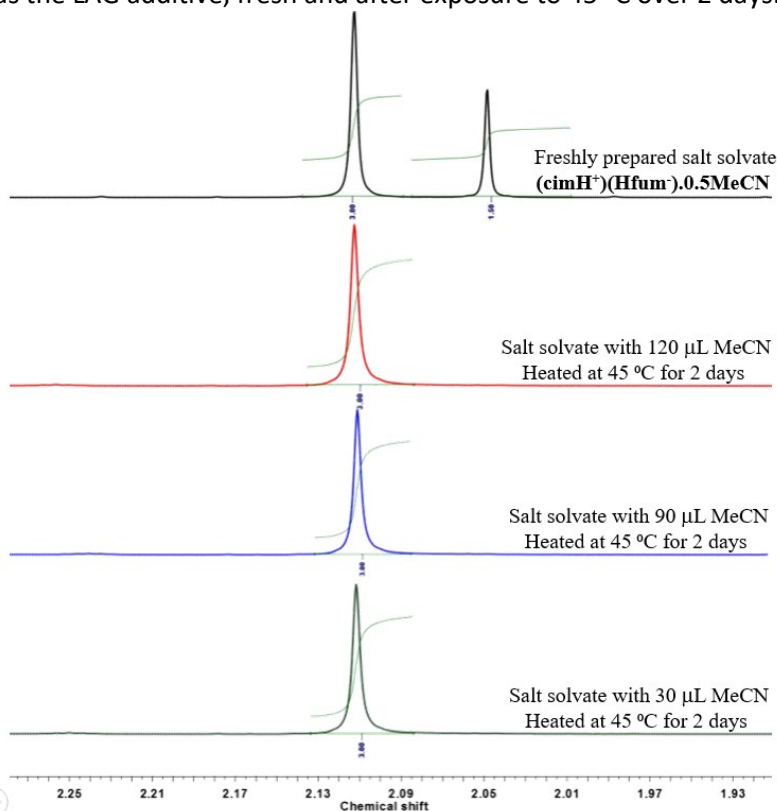


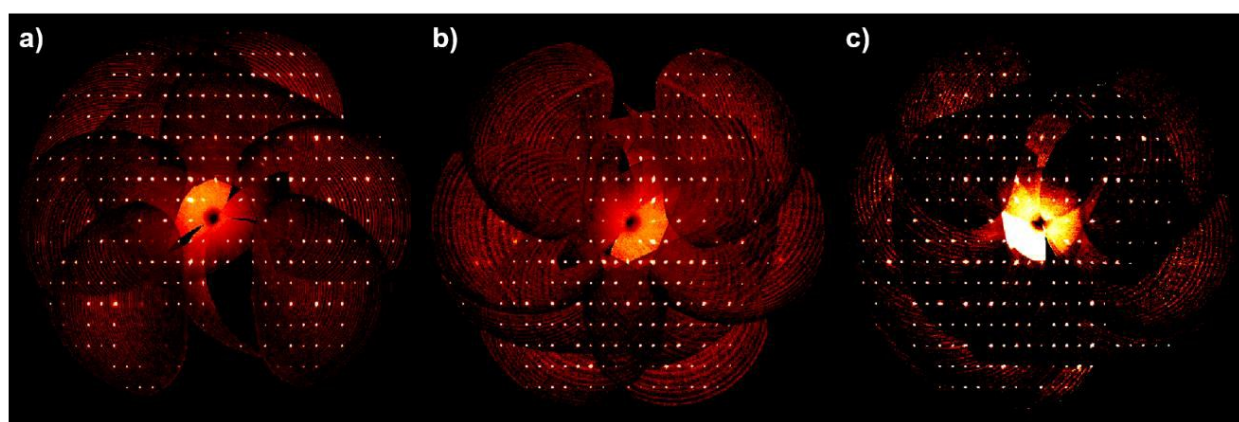
Figure S11. Comparison of ^1H NMR solution spectra for (top to bottom): a sample of freshly prepared **1** and samples of **1** prepared by using different amounts of MeCN as the milling liquid, after exposure to 45 $^{\circ}\text{C}$ over 2 days.

Table S1. Quantitative comparison of the particle size and MeCN content for differently prepared and treated samples of **1**.

Type of material	Treatment	longest particle dimension	Mole ratio
Single crystals	Before treatment	1.2 mm	0.50
	After treatment ^a	1.2 mm	0.49
	Gently ground after treatment	230 μm	0.25
	Thoroughly pulverized after treatment ^a	19 μm	0.11
Powder	Mechanochemically	228 nm	0.50
	Mechanochemically after treatment ^a	228 nm	none

^adesolvation conditions are after 45 °C, 2 days**Table S2.** Crystallographic data for a crystal of **1**, (cimH⁺)(Hfum⁻)-0.5MeCN, before and after exposure to 45 °C.

Unit cell parameters	<i>a</i> (Å)	<i>b</i> (Å)	<i>c</i> (Å)	β (Å)	<i>V</i> (Å ³)
before heating	13.8039(12)	8.0191(7)	18.7153(16)	107.580(2)	1974.93
after heating (day=5)	13.7985(12)	8.0172(7)	18.7226(17)	107.657(3)	1973.62
after heating (day=10)	13.7920(11)	8.0148(7)	18.7259(16)	107.555(3)	1973.56

**Figure S12.** Diffraction images collected in the 0kl plane for the single crystals a) freshly prepared, b) heated at 45°C for five days, and c) heated at 45°C for ten days.

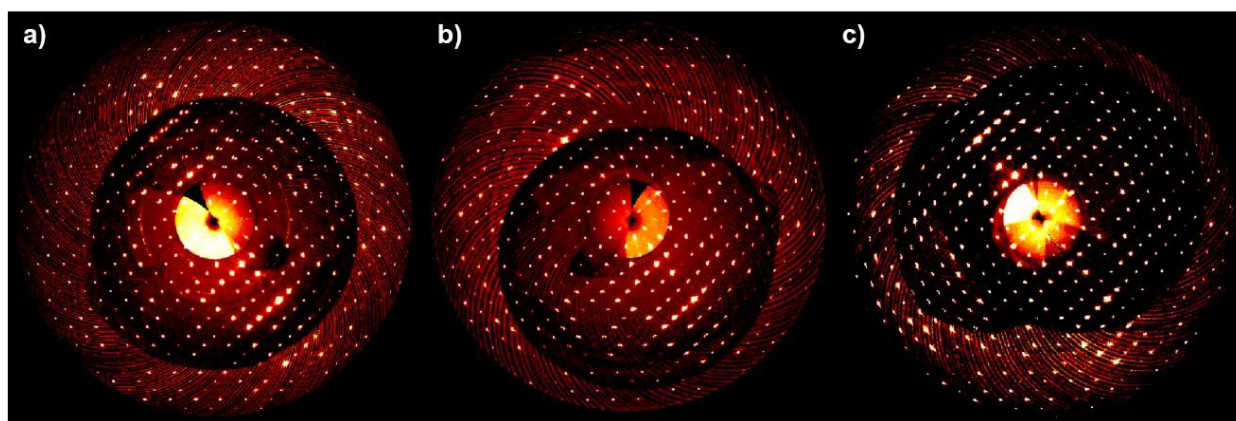


Figure S13. Diffraction images collected in the $h0l$ plane for the single crystals a) freshly prepared, b) heated at 45°C for five days, and c) heated at 45°C for ten days.

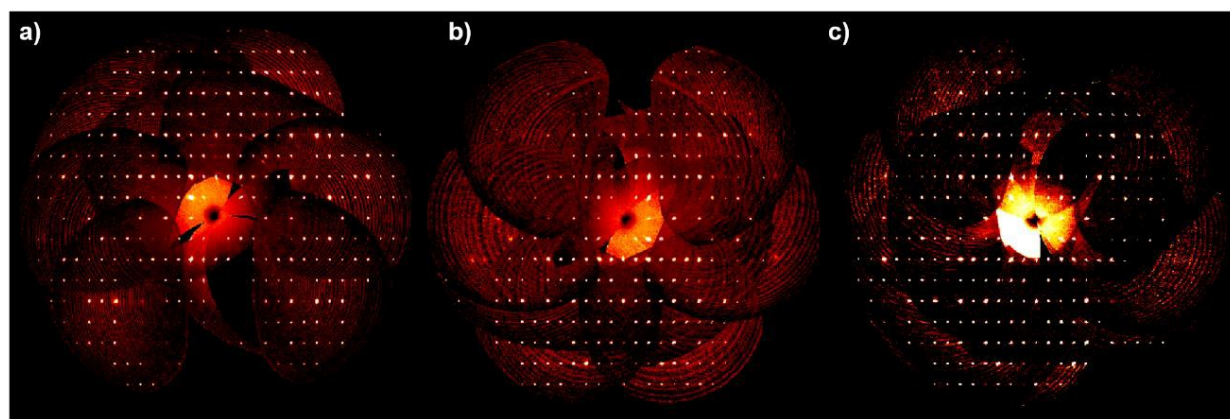


Figure S14. Diffraction images collected in the $hk0$ plane for the single crystals a) freshly prepared, b) heated at 45°C for five days, and c) heated at 45°C for ten days.

[†] G.M. Sheldrick. *Acta Cryst.* 2015, **C71**, 3-8